A Modern Control Theory Based Algorithm for Control of the NASA/JPL 70-Meter Antenna Axis Servos

R. E. Hill

Ground Antennas and Facilities Engineering Section

A digital computer-based state variable controller has been designed and applied to the 70-m antenna axis servos. The general equations and structure of the algorithm and provisions for alternate position error feedback modes to accommodate intertarget slew, encoder referenced tracking, and precision tracking modes are described. Development of the discrete time domain control model and computation of estimator and control gain parameters based on closed loop pole placement criteria are discussed. The new algorithm has been successfully implemented and tested in the 70-m antenna at Deep Space Station (DSS) 63 in Spain.

I. Introduction

Servo design studies utilizing dynamic models of the new 70-m antenna structures identified many changes in control dynamics which result from the antenna upgrade from 64 m to 70 m [1]. These studies indicated that the 64-m rate loop hardware and software required only minor parameter value modifications when upgraded to the 70-m system. The 70-m Antenna Servo Controller employs a software pointing control algorithm similar to that used in the previous 64-m antenna configuration. This article describes the new servo control algorithm and the analytic servo design methods employed in deriving the control coefficient values for the new 70-m antenna.

II. Control Algorithm Description

The position control loop is closed in the Antenna Servo Control (ASC) computer by a digital, state variable controller based on modern feedback control techniques. It employs feedback of the hardware system state variables to achieve the required closed loop system performance. A linear estimator, or observer, provides a measure of those states which are not instrumented. The state variable feedback controller differs from the classical feedback controller, which relied on the use of cascade networks (implemented in either hardware or software) to provide the necessary servo compensation.

The state variable controller has several advantages: (1) its compensation techniques are not limited to the use of physically realizable networks; (2) the state variable approach facilitates discrete time domain design methods, resulting in efficient utilization of the control computer; (3) the state estimator provides an accurate, low-noise measure of rate and acceleration; (4) the estimator provides a powerful method of encoder data error detection and correction which permits uninterrupted operation during brief intervals when the encoder data are unusable; and (5) the state variable method

employs a standardized matrix representation of the system which is convenient for digital computer processing. The closed loop state variable controller has the linear system properties of a classical linear feedback controller, and its performance is related to bandwidth and linear error coefficients.

The operation of the control algorithm is illustrated in the block diagram of Fig. 1, which depicts a single axis of the two-axis Azimuth/Elevation system. The block labeled "Antenna Hardware" represents the control electronics, the rate loop, and the output gear ratio. Its output, X, is a vector whose elements represent the individual system states. The hardware control input, U, corresponds to the rate command input to the hardware generated by the control algorithm. Antenna position is sensed by a bull gear referenced angle encoder and also by an optical autocollimator. These devices are represented by two additional blocks, both having the input state vector X. The autocollimator detects antenna position error relative to a Precision Instrument Mount or Master Equatorial (ME) which serves as a precision tracking position reference and is controlled in celestial hour angle and declination coordinates. The sensing axes of the autocollimator are precisely aligned with respect to the geometric axis of the antenna primary reflector, thus providing more precise pointing than is available from axis mounted angle encoders.

The representative equation of the "Antenna Hardware" block is the generalized difference equation relating the hardware state vector at the discrete times of the computer sampling to the state vector's previous value and to the control input, U. The discrete transition matrix, Φ, and the input vector, Γ, describe the dynamic behavior of the physical system. The angle encoder and the autocollimator are represented by vectors H_E and H_A, which operate on the state vector, X, and produce the scalar azimuth (or elevation) encoder angle and autocollimator angle error.

The software estimator computes the antenna state variables for subsequent processing and feedback to the hardware control input. The estimator is essentially a dynamic simulation of the physical antenna and has the same input and difference equation as the hardware. Under ideal conditions, the estimator output state vector, E, is identical to the antenna state vector, X. Errors in the estimated state vector, E, arise from modeling errors and from uncompensated disturbances. These errors are corrected by a comparison of the estimated with the true values of the encoder angle, and feedback of the estimator error, Y_E, with a feedback gain factor, L.

The feedback of the estimator error introduces a feedback loop around the estimator with a dynamic response governed by the amount of correction (gain) in the loop. By proper selection of the estimator correction coefficients, L, the speed

of correction of erroneous estimates (and also the speed of response to transient invalid encoder data) can be adjusted. The coefficients are therefore designed to reach a compromise between rapid estimator error corrections and encoder data noise filtering.

A logical test on the size of the estimator error provides a powerful method of detecting gross errors in encoder reading. The omission of the estimator correction when such errors are detected is equivalent to substituting the estimated value for the real encoder value and thus provides an optimal filter of gross errors. The limits on such a test must be sufficiently wide to permit recovery after an interval of rejecting erroneous data. Estimator errors due to modeling and disturbances will tend to accumulate during periods of invalid data and could prevent the acceptance of valid data if the limits are too restrictive. A dynamic limit test, with time and rate dependent limits calculated to accommodate cumulative error, has been considered but not yet implemented.

The servo feedback loop is closed by multiplying the state estimate, E, by a feedback gain, K. Because the estimate, E, is approximately equal to the hardware output, X, the result is an effective feedback loop around the physical hardware. The dynamic properties of the closed servo loop are hence controlled by the value of K. The input to the software rate/acceleration limiter is

$$U = N \cdot R - K \cdot E \qquad (1)$$

where R is the input command, N is the input gain constant, and $K \cdot E$ is the scalar product which when expanded yields

$$U = N \cdot R - K_1 \cdot E_1 - K_2 \cdot E_2 - K_3 \cdot E_3 - \cdots - K_6 \cdot E_6 \qquad (2)$$

The input gain, N, controls the overall gain of the servo and is assigned different values according to the mode of operation.

The individual elements of gain vector K correspond to integral error, position, rate, acceleration, and other gains, and thus determine the closed loop stiffness and dynamic response of the servo. The K values are assigned to achieve the desired linear system performance. The method of computation of the K values is described in detail in Section V.

III. Modes of Operation

A. Computer Small Error Mode

In the Computer Small Error Mode the servo is configured as described above in Section II to provide linear type II posi-

tion servo performance. This mode is employed when position control utilizing feedback from the axis encoders is required. The rate command is computed according to Eq. (2) and the input gain, N, is set equal to K_2 to provide unity position gain. Automatic transfer to the "Large Error" mode occurs any time conditions which would result in prolonged control saturation occur. A simple test initiates the transfer any time the calculated control input, U, exceeds 1.5 times the software rate limit.

B. Precision Mode

In the Precision Mode, the Az/El servo tracks the position of the Master Equatorial (ME), as contrasted to the Computer Small Error Mode where positioning to a specific encoder angle is required. The angular difference between the antenna and the ME is detected by a two-axis optical autocollimator mounted on the antenna. A single axis of the autocollimator is depicted in Fig. 1 as a hardware block with inputs from both the (Az/El) hardware and the Master Equatorial. The autocollimator output is filtered by a 2-pole low pass filter in the hardware. In software, the azimuth error signal is multiplied by the approximate secant of the elevation angle to correct for the elevation-dependent geometry of the autocollimator reflected light path.

Precision Mode position control is accomplished through an alternate branch in the software which evaluates control and estimator equations modified to use autocollimator derived position error in place of the position command, R, and the estimated encoder angle E_2. The modified estimator equations compute integral error based on the filtered autocollimator error, as contrasted to the encoder vs command angle error which is used in the computer mode. In the Precision Mode the input to the software rate/acceleration limiter becomes

$$U = -K_1 \cdot E_1 - K_2 \cdot \epsilon_P - K_3 \cdot E_3 - \cdots - K_6 \cdot E_6 \quad (3)$$

The modified control and estimator equations provide type II control using the autocollimator error for position and integral control with damping provided by the estimator. A distinct advantage of this configuration over true error-only control is the continuity of the estimator equations between the computer and precision modes. Since the integral error estimate, E_1, changes relatively slowly, there is no abrupt change in the estimator output resulting from mode to mode transitions. Mode transfer settling times are thus minimized.

The software employs a four-pole minimum Integral Time Absolute Error (ITAE) low pass digital filter to restrict the error signal bandwidth and eliminate signal components resulting from deflections of the alidade structure. The filter bandwidth of 2.86 Hz was adjusted empirically on the 64-m

antenna to provide the best damping of the alidade structure and to minimize the effects of autocollimator noise.

C. Large Error Mode

To prevent saturation of the type II servo loop, a third mode of operation is provided with software controlled mode selection. A Large Error Mode of operation is provided to accommodate intertarget slew motions and any other transient conditions which would saturate the type II servo and cause large excursions of position error.

In the Large Error Mode the software configuration is altered slightly from the computer mode configuration to provide slew rate control with smooth rate transitions. The estimator functions the same as in the Small Error Mode except that all of the estimator elements are not utilized in the control. The control gain, K, is chosen to produce a slow response rate servo with the bandwidth selected to limit the peak acceleration in response to a maximum rate step input. This type of control was chosen to minimize acceleration transients which would excite oscillations of the antenna structure. In this mode the first two elements of K, which correspond to integral error and position feedback gain, are set to zero. The remaining elements are selected to achieve the desired closed loop servo bandwidth. In the Large Error Mode, the command input, R, is a rate signal value computed to reposition the antenna to the desired angle in minimum time. The input gain, N, is set equal to a function of K_3, K_4, K_5, K_6 to provide unity rate servo gain.

The software transfers from Large Error to Computer Small Error control when both the rate error and position error are sufficiently small to permit unsaturated type II servo performance. The limits for transfer are 0.05 degree/s rate error and 0.03 degree position error. Upon initial entry into Small Error control, the integral angular position error estimate, E_1, is initialized to a value proportional to the estimated rate. This helps to minimize the error settling time. The mode control logic permits entry into Precision Mode only from the Computer Small Error Mode.

IV. Control Algorithm Sequencing and Timing

The computations of the discrete system matrices and of the feedback gains are based on a specific (50 ms) sample interval and negligible time delay between each encoder input and the corresponding rate command output. These conditions are satisfied by the use of timed interrupt driven software with lower priority interrupts masked during execution of time critical control computations. Time skew errors are minimized by assigning highest priority to a 100 pps interrupt which ini-

tiates encoder read and control computation at regular 50 ms intervals. Computing time effects are minimized by consecutive sequencing of the Azimuth and Elevation axis functions with the Elevation read and compute operations beginning 20 ms behind those for Azimuth. This 20 ms offset allows sufficient time for completion of the Azimuth computations.

The estimator is initialized prior to antenna brake release by equating the angular position estimate to the encoder reading and by setting all other state estimates to zero. On the transition from the Large Error to Small Error mode the integral position error estimate is initialized to a value proportional to the estimated rate. The estimator is not reinitialized on transitions to or from the Precision Mode.

V. Computation of the Control Algorithm Coefficients

A. Linear System Matrices F and G

The simplest linear dynamic model of the 70-m Az/El antenna assumes a rigid body structure with the moment of inertia dominated by that of the inertia wheels attached to the motor shafts. The compressibility of the hydraulic oil and its piping combined with the inertia result in a complex conjugate pole pair. Two real, open-loop poles corresponding to the rate loop compensation networks are also modeled. With the two integrations operating on the angular rate and position to produce position and integral error, the order of the dynamic system for control becomes six. Because estimator feedback is based on encoder angle, the integral error is an unobservable state and is excluded from the estimator design process. It is introduced later in the control gain design process.

The simplified structure model described above was used in the design of the MK IV 64-m antenna servos. However, because of the significant dynamics changes resulting from the structure additions for the 70-m antenna, a more comprehensive structure model was needed. The new model [1] includes gear reducer stiffness, three tipping structure modes, and two alidade modes in Elevation. The resulting closed rate loop model is 10th order for Azimuth and 14th order for Elevation. The low frequency closed rate loop poles of these models differ considerably from those computed from the simplified rigid body structure model even though the rigid body inertia includes the static inertia of the structure. This difference results from the finite compliance of the gear reducers and of the structure. The models for both the 70-m and 64-m structures indicate the Elevation axis compliance is dominated by the alidade.

Because of the uncertain degradation of robustness associated with errors in modeling the structure, a decision was

made to reduce the new model to the sixth order in the form of the simplified model described earlier. The underlying assumption, that system robustness resulting from the use of a rigid body based model is superior to that from a higher degree structure model, has not been investigated. The reduction was accomplished by deleting the higher frequency pole-zero pairs associated with the structure modes. The remaining hydraulic motor and compensation network poles and zeros were then combined with the rate-to-position-to-integral-error integrations to synthesize the sixth order model.

The poles and zeros for the Azimuth and Elevation closed rate loops are listed in Table 1, and their corresponding linear system matrices are in Table 2. In the linear system matrices the value of 20 in the first row results from normalization of the integral error with respect to the sampling time interval. This produces a value of unity in the discrete transition matrix and helps to reduce estimator computation time. Further simplifications are accomplished by replacing the negligibly small elements in the first row of the transition matrix and the first element of the input matrix with zeros. The resulting coordinate skew corrupts the integral estimate by less than 12.5 microdegree-seconds in the worst case.

The input large error mode gain constants, N, are calculated from the linear system matrices for the condition of unity rate gain. The results for azimuth are expressed by

$$N = 1.0 + K_3 + 5.173\,K_5 + 10.001\,K_6 \qquad (4)$$

and for elevation

$$N = 1.0 + K_3 + 9.041\,K_5 + 17.479\,K_6 \qquad (5)$$

B. The Discrete Transition and Input Matrices

The linear system matrices F and G are transformed from the continuous time domain to the discrete (sampled data) time domain to produce the discrete transition matrix, Φ, and the discrete input matrix, Γ. A computer sampling time interval of 50 ms (20 samples/s) was selected, as it satisfies the criteria of (1) negligible pointing error resulting from sampling effects at maximum tracking rate and acceleration; (2) the rate exceeds 10 times the required closed position loop bandwidth; and (3) the rate being a convenient multiple of the DSN frequency and timing standard 100 pps signals. The third criterion derives from the necessity to synchronize the tracking position commands to the Deep Space Network clock.

Using the conversions for sampling described by a zero order hold with no delay

$$\Phi = \text{expm} (F * T) \qquad (6)$$

$$\Gamma = \Psi * T * G \qquad (7)$$

where expm denotes the matrix exponential function.

The Ψ matrix is obtained from the relationship

$$F * T * \Psi = \Phi - I \qquad (8)$$

where I is the identity matrix.

A Fortran program was developed to evaluate Φ, Ψ, and Γ from the continuous time system matrices, F and G, and sampling time, T, using the scale and square method described by Moler and Van Loan [4]. The numerical results for ϕ and Γ are listed in Table 3.

The control gain vector, K, and the estimator gain L are calculated by the method of closed loop eigenvalue assignment. This method, also referred to as pole placement, combines the desired closed loop pole locations with the discrete system matrices Φ and Γ in the Ackerman [3] equations to produce the control feedback gain, K, or estimator gain, L.

The specified pole locations were iterated to insure satisfactory robustness and insensitivity to computational roundoff and to angle encoder quantizing. Deadbeat response (minimum settling time) is impractical because it requires excessive control effort to overcome small disturbances. The following general criteria were employed in specifying closed loop pole locations:

(1) The two lowest frequency poles are specified to achieve the desired bandwidth and settling time. For optimal error settling time (ITAE criteria) [2], these poles are complex conjugates with equal real and imaginary parts. Assigning more than two dominant poles using the ITAE criteria, the Butterworth criteria, or (presumably) a similar criterion tends to increase the transient overshoot of the closed loop system and is avoided. The bandwidth of the estimator is always at least three times that of the overall system and narrow enough to provide a level of noise filtering.

(2) Other low frequency poles may be specified to cancel open loop zeros in order to produce a flat closed loop low frequency response.

(3) High frequency poles are specified near their corresponding open loop locations to minimize the value of the resulting K or L. Estimator poles should be dis-

placed slightly from the control poles to enhance robustness.

(4) The resulting values of K or L are reviewed for suitably large values of elements corresponding to integral error, position, and rate, and for small values of the remaining elements, and the pole specifications are adjusted accordingly. The control input, U, and the subsequent encoder position change resulting from single least significant bit changes of the encoder output are evaluated from the K·L and Γ·K·L scalar products, respectively. In general, the estimate accuracy of those states not closely coupled to the output state tends to diminish with remoteness of coupling. Therefore, noise and wasted control effort are reduced as less control authority is assigned to those states.

Tables 4 through 6 list the values of the closed loop S plane poles used in the 70-m controller design and the resulting control gain, K, and estimator feedback gain, L. The estimator gain is computed from the 5th-order discrete system matrices to avoid the unobservable integral error. Dimensional consistency with Φ is obtained by expanding L to the sixth order with the addition of a zero value first element. Thus Table 5 lists six L coefficients but only 5 estimator poles.

VI. Summary

The control algorithm along with the parameter values described above were incorporated in the system software and tested successfully in the 70-m antenna at DSS 63 in Spain.

VII. Areas for Further Investigation

The degree of system performance improvement to be gained from the use of higher-order structure models has not yet been investigated. As discussed in Section V.A, only the zero order approximation of the structure was utilized in the present work because of robustness concerns. Comparison of the models of Table 1 with those of Table 6 and Figs. 5 and 6 of [1] shows that significant dynamics are neglected in the sixth-order model. The potential improvement of both estimator accuracy and structure damping can be expected to peak at some level of model complexity. Beyond this peak, estimator noise and system robustness are expected to degrade due to modeling errors and unmodeled nonlinearities. Further work can utilize current known values of the nonlinearities, structure dynamics test data, and estimates of modeling errors.

References

[1] R. E. Hill, "A New State Space Model for the NASA/JPL 70-Meter Antenna Servo Controls," *TDA Progress Report 42-91*, vol. July–September 1987, Jet Propulsion Laboratory, Pasadena, California, November 15, 1987.

[2] A. E. Bryson and Y. C. Ho, *Applied Optimal Control*, Washington, D.C.: Hemisphere Publishing, 1975.

[3] G. F. Franklin and J. D. Powell, *Digital Control of Dynamic Systems*, Reading, Massachusetts: Addison-Wesley, 1981.

[4] C. Moler and C. Van Loan, "Nineteen Dubious Ways to Compute the Exponential of a Matrix," *SIAM Review*, vol. 20, no. 4, pp. 801–836, October 1978.

Table 1. Poles and zeros of the closed rate loop model, 70-m antenna

Axis	Poles	Zeros
Azimuth	$0.00 \pm j \ 0.00$	
	$-1.45 \pm j \ 0.0$	$-2.2 \pm j \ 0.00$
	$-60.80 \pm j \ 0.00$	$-81.0 \pm j \ 0.00$
	$-7.81 \pm j \ 13.01$	
Elevation	$0.00 \pm j \ 0.00$	
	$-1.45 \pm j \ 0.00$	$-2.2 \pm j \ 0.00$
	$-37.70 \pm j \ 0.00$	$-81.0 \pm j \ 0.00$
	$-20.81 \pm j \ 16.44$	

Table 2. Linear system matrices for 70-m rate loops

Azimuth axis

$$F = \begin{bmatrix} 0 & 20 & 0 & 0 & 0 & 0 \\ 0 & 0 & 1 & 0 & 0 & 0 \\ 0 & 0 & 0 & 15.17 & 0 & 0 \\ 0 & 0 & -15.17 & -15.62 & 1 & 1 \\ 0 & 0 & 0 & 0 & -1.45 & 0.75 \\ 0 & 0 & 0 & 0 & 0 & -60.8 \end{bmatrix}$$

$$G = \begin{bmatrix} 0 \\ 0 \\ 0 \\ 0 \\ 0 \\ 608 \end{bmatrix} \qquad H = \begin{bmatrix} 0 \\ 1 \\ 0 \\ 0 \\ 0 \\ 0 \end{bmatrix}$$

Elevation axis

$$F = \begin{bmatrix} 0 & 20 & 0 & 0 & 0 & 0 \\ 0 & 0 & 1 & 0 & 0 & 0 \\ 0 & 0 & 0 & 26.52 & 0 & 0 \\ 0 & 0 & -26.52 & -41.62 & 1 & 1 \\ 0 & 0 & 0 & 0 & -1.45 & 0.75 \\ 0 & 0 & 0 & 0 & 0 & -37.7 \end{bmatrix}$$

$$G = \begin{bmatrix} 0 \\ 0 \\ 0 \\ 0 \\ 0 \\ 659 \end{bmatrix} \qquad H = \begin{bmatrix} 0 \\ 1 \\ 0 \\ 0 \\ 0 \\ 0 \end{bmatrix}$$

Table 3. Discrete system matrices, 70-m antenna (sample interval, $TS = 0.0500$ s)

Azimuth discrete transition matrix, Φ

$$
\begin{bmatrix}
0.100000E+01 & 0.100000E+01 & 0.239851E-01 & 0.000000E+00 & 0.000000E+00 & 0.000000E+00 \\
0.000000E+00 & 0.100000E+01 & 0.461185E-01 & 0.141961E-01 & 0.251086E-03 & 0.136192E-03 \\
0.000000E+00 & 0.000000E+00 & 0.784645E+00 & 0.477875E+00 & 0.138320E-01 & 0.610394E-02 \\
0.000000E+00 & 0.000000E+00 & -.477875E+00 & 0.292594E+00 & 0.301792E-01 & 0.772115E-02 \\
0.000000E+00 & 0.000000E+00 & 0.000000E+00 & 0.000000E+00 & 0.930066E+00 & 0.111487E-01 \\
0.000000E+00 & 0.000000E+00 & 0.000000E+00 & 0.000000E+00 & 0.000000E+00 & 0.478353E-01
\end{bmatrix}
$$

Azimuth discrete input matrix, Γ

$$
\begin{bmatrix}
0.000000E+00 \\
0.122145E-02 \\
0.828046E-01 \\
0.244640E+00 \\
0.250242E+00 \\
0.952165E+01
\end{bmatrix}
$$

Elevation discrete transition matrix, Φ

$$
\begin{bmatrix}
0.100000E+01 & 0.100000E+01 & 0.225781E-01 & 0.000000E+00 & 0.000000E+00 & 0.000000E+00 \\
0.000000E+00 & 0.100000E+01 & 0.413012E-01 & 0.162868E-01 & 0.321490E-03 & 0.209996E-03 \\
0.000000E+00 & 0.000000E+00 & 0.568074E+00 & 0.417450E+00 & 0.158207E-01 & 0.861108E-02 \\
0.000000E+00 & 0.000000E+00 & -.417450E+00 & -.870649E-01 & 0.148759E-01 & 0.394712E-02 \\
0.000000E+00 & 0.000000E+00 & 0.000000E+00 & 0.000000E+00 & 0.930066E+00 & 0.161014E-01 \\
0.000000E+00 & 0.000000E+00 & 0.000000E+00 & 0.000000E+00 & 0.000000E+00 & 0.151829E+00
\end{bmatrix}
$$

Elevation discrete input matrix, Γ

$$
\begin{bmatrix}
0.000000E+00 \\
0.212184E-02 \\
0.138387E+00 \\
0.213978E+00 \\
0.350851E+00 \\
0.148261E+02
\end{bmatrix}
$$

Table 4. Estimator gain coefficients, L

Axis	L_1	L_2	L_3	L_4	L_5	L_6	S plane poles			
Azimuth	0.0000	0.7398	5.1375	−7.7241	3.2878	−.0252	−2.00 ± j 0.00	−8.00 ± j 0.00	−17.0 ± j 17.0	−60.8 ± j 0.00
Elevation	0.0000	0.5711	7.3192	−13.4937	5.1036	0.0001	−2.00 ± j 0.00	−8.00 ± j 0.00	−25.0 ± j 25.0	−37.7 ± j 0.00

Table 5. Azimuth control gain coefficients, K

Mode	K_1	K_2	K_3	K_4	K_5	K_6	S plane poles			
Computer small error	0.0156	0.6863	−.2312	0.0141	0.0586	−.0318	−2.20 ± j 0.00	−.50 ± j 0.50	−10.0 ± j 0.00	−12.0 ± j 12.0
Computer small error, alternate	0.0302	0.9863	−.2013	0.0397	0.0598	−.0307	−2.20 ± j 0.00	−.70 ± j 0.70	−10.0 ± j 0.00	−12.0 ± j 12.0
Precision	0.0071	0.3590	−.3287	−.1367	0.0448	−.0453	−2.20 ± j 0.00	−.45 ± j 0.45	−5.0 ± j 0.00	−12.0 ± j 12.0
Large error	0.0000	0.0000	0.4955	−.5467	−.0389	−.1270	−0.00 ± j 0.00 −8.0 ± j 0.00	−.00 ± j 0.00	−2.2 ± j 0.00	−2.0 ± j 2.0

Table 6. Elevation control gain coefficients, K

Mode	K_1	K_2	K_3	K_4	K_5	K_6	S plane poles			
Computer small error	0.0281	0.9153	0.2593	0.2987	0.0136	−.0368	−2.20 ± j 0.00	−.70 ± j 0.70	−8.00 ± j 0.00	−18.0 ± j 18.0
Computer small error, alternate	0.0564	1.3565	0.2791	0.3047	0.0153	−.0351	−2.20 ± j 0.00	−1.00 ± j 1.00	−8.00 ± j 0.00	−18.0 ± j 18.0
Computer small error, alternate	0.0310	0.8229	0.2751	0.3508	0.0048	−.0454	−2.20 ± j 0.00	−1.00 ± j 1.00	−4.00 ± j 0.00	−18.0 ± j 18.0
Computer small error, alternate	0.0145	0.6370	0.2469	0.2952	0.0125	−.0379	−2.20 ± j 0.00	−.50 ± j 0.50	−8.00 ± j 0.00	−18.0 ± j 18.0
Precision	0.0050	0.2612	0.2602	0.3707	−.0017	−.0519	−2.20 ± j 0.00	−.45 ± j 0.45	−3.00 ± j 0.00	−18.0 ± j 18.0
Large error	0.0000	0.0000	2.1903	1.1171	−.0869	−.1358	−0.00 ± j 0.00 −20.0 ± j 0.00	−.00 ± j 0.00	−2.20 ± j 0.00	−2.0 ± j 2.0

NOTES:

1) K_C, N_C COMPUTER MODE CONSTANTS, ZERO EFFECTIVE VALUE IN OTHER MODES

2) K_{LG}, N_{LG} LARGE ERROR MODE CONSTANTS, ZERO EFFECTIVE VALUE IN OTHER MODES

3) K_P PRECISION MODE GAIN CONSTANT, ZERO EFFECTIVE VALUE IN OTHER MODES

AXIS ENCODER H_E

H_A

M-E POSITION

AUTOCOLLIMATOR

ANTENNA HARDWARE DYNAMICS
$X(n+1) = \Phi X(n) + \Gamma U_P$

X

U_P

HARDWARE RATE/ ACCELERATION LIMITER

D/A CONVERTER

A/D CONVERTER

PARALLEL INTERFACE

SOFTWARE HARDWARE

COMPUTED RATE COMMAND U

DIGITAL FILTER

SECANT CORRECTION AZIMUTH ONLY

SOFTWARE RATE/ ACCELERATION LIMITER

Σ

N_{LG}

N_C

K_{LG}

K_C

K_P

E

LARGE ERROR LOGIC AND EQUATIONS

POSITION COMMAND INPUT, R

STATE ESTIMATOR
$E(n+1) = \Phi E(n) + \Gamma U + L Y_E$
$E_1(n+1) = E_1(n) + E_2(n)$ COMPUTER MODE
$E_1(n+1) = E_1(n) + \epsilon_P$ PRECISION MODE

ϵ_P

H_E

AUTOCOLLIMATOR POSITION ERROR
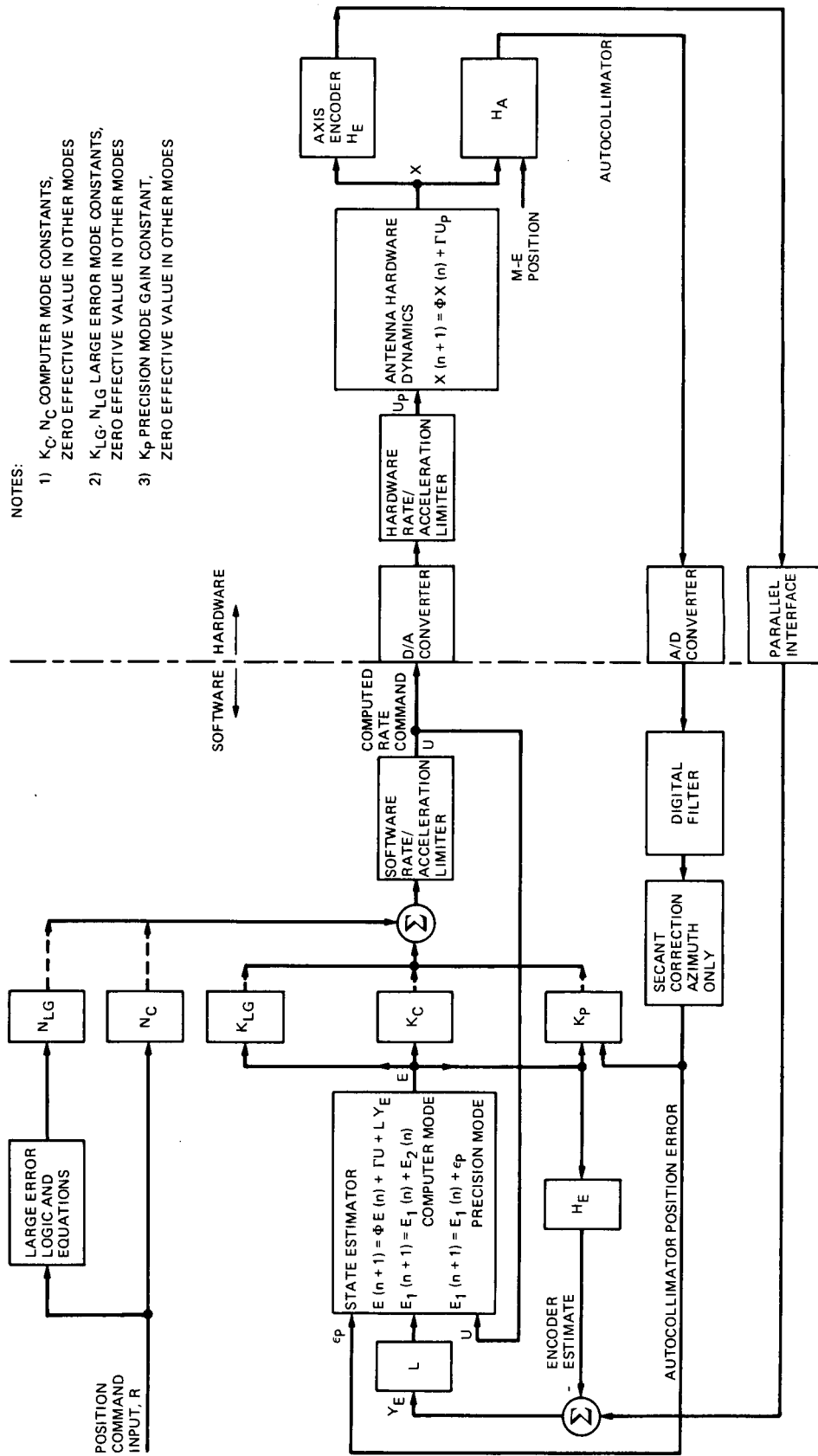
L

Y_E

U

ENCODER ESTIMATE

Σ

Fig. 1. Block diagram for 70-m antenna servo control algorithm